Induced seismicity in North-Central Oklahoma, a spatial and meta-data analysis

Shan Ye, Tyler Tripplehorn, Nam Pham

I) Introduction:

The number of earthquakes in Oklahoma has increased significantly since 2009. Many papers (e.g. Walsh III and Zoback 2015, Langenbruch and Zoback 2016, McNamara et al. 2015) have been investigating the relationship between wastewater injection and earthquakes. The papers series of Zoback group describe clearly the spatial relationship between injection wells and earthquakes. In our project, we want to extend the work of Brizendine (2016) in using Phi-H values to better understand the porosity distribution of the Arbuckle group and if there is any relationship between porosity distributions and earthquakes in Oklahoma. The final goal is to help Oklahoma Cooperation Committee determine whether there is a safe injection volume for the oil and gas companies.

II) Geologic Background:

The area of interest contains three major geologic provinces: the Anadarko Shelf, the Cherokee Platform, and the Anadarko Basin (Northcutt and Campbell, 1996). The Cherokee region is separated from the Anadarko region by the Central Oklahoma Fault Zone and the Nemaha Ridge (Northcutt and Campbell, 1996). The area is underlain by pre-Cambrian basement rocks composed of granites dating to about 1.4 Ga (Johnson, 2008). A major unconformity separates the basement rocks from the Phanerozoic sedimentary cover. During the Cambrian and

Ordovician Periods the region was flooded resulting in the deposition of primarily thick units of dolomites with interspersed sections of sandstones, limestone and shales (Johnson, 2008). It was during this time that the Arbuckle Group was deposited. It ranges in thickness from 1000-2000 ft in the study area with the thinner values located in the north and thickening to the south (Johnson, 2008). Continued transgression and regression of seas resulting in intermittent intervals of deposition and erosion within the study area continued until a major uplift and tilting event of northeastern Oklahoma resulted in widespread erosion and the placement of the Woodford unconformity (Huffman, 1958). After deposition of the Woodford formation, transgressing seas deposited the Kinderhook Shale and the Osagean "Mississippi lime" (Berryhill, 1961). The Mississippi lime is the primary dewatering play in Oklahoma and makes up the vast bulk of the wastewater injection volumes disposed of in injection wells. The tectonics of the region remained relatively stable until the Late Mississippian to Early Pennsylvanian when a major orogenic event took place in the south (Eardley, 1951). This tectonic pulse caused the formation of the Central Oklahoma Arch and the Nemaha Ridge which now serve as a boundary between the eastern and western portions of our study area (Eardley, 1951).

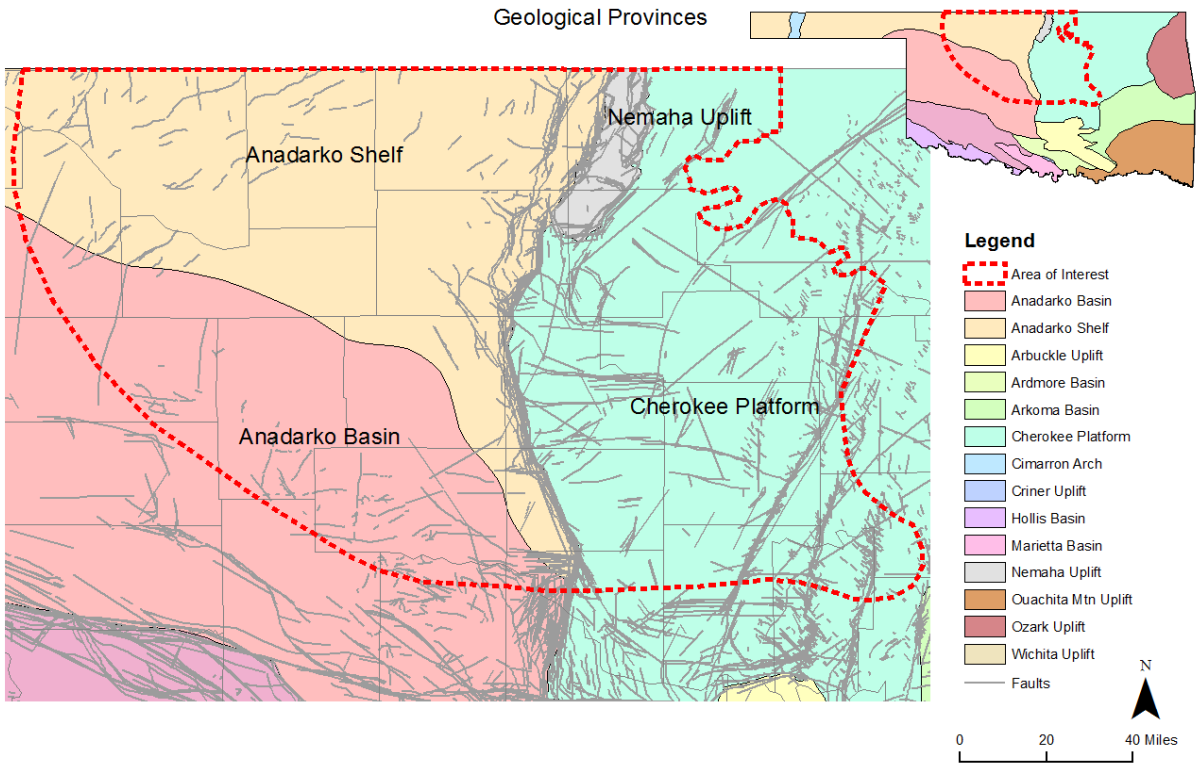

Figure 1: Geological Provinces of the study area

III) Data:

We digitized the map of the area of interest in the report from the Oklahoma Cooperation Committee released in February 2017 (http://www.occeweb.com/News/2017/02-24-17%20FUTURE%20DISPOSAL.pdf)

and used the area defined in the report as our study area (Figure 2). Our study area is comprised of two parts: the Western (OWRA) and Central (OCRA) regions that are separated by the Nemaha Fault Zone. The area of interest is further divided into five study zones which are based on the research of Walsh and Zoback (2015). We also generated equal-area squared grids with

various lateral lengths ranging from 10 miles to 90 miles. Well location data was obtained from the IHS Enerdeq Browser and well logs were gathered from MJ Systems. Earthquake records for Oklahoma were obtained from the Earthquake Catalog of the USGS's Earthquake Hazards Program (https://earthquake.usgs.gov/earthquakes/search/). Wastewater injection locations and volumes for Class II injection wells were obtained from yearly reports administered by the Oklahoma Corporation Commission (http://www.occeweb.com/og/ogdatafiles2.htm).

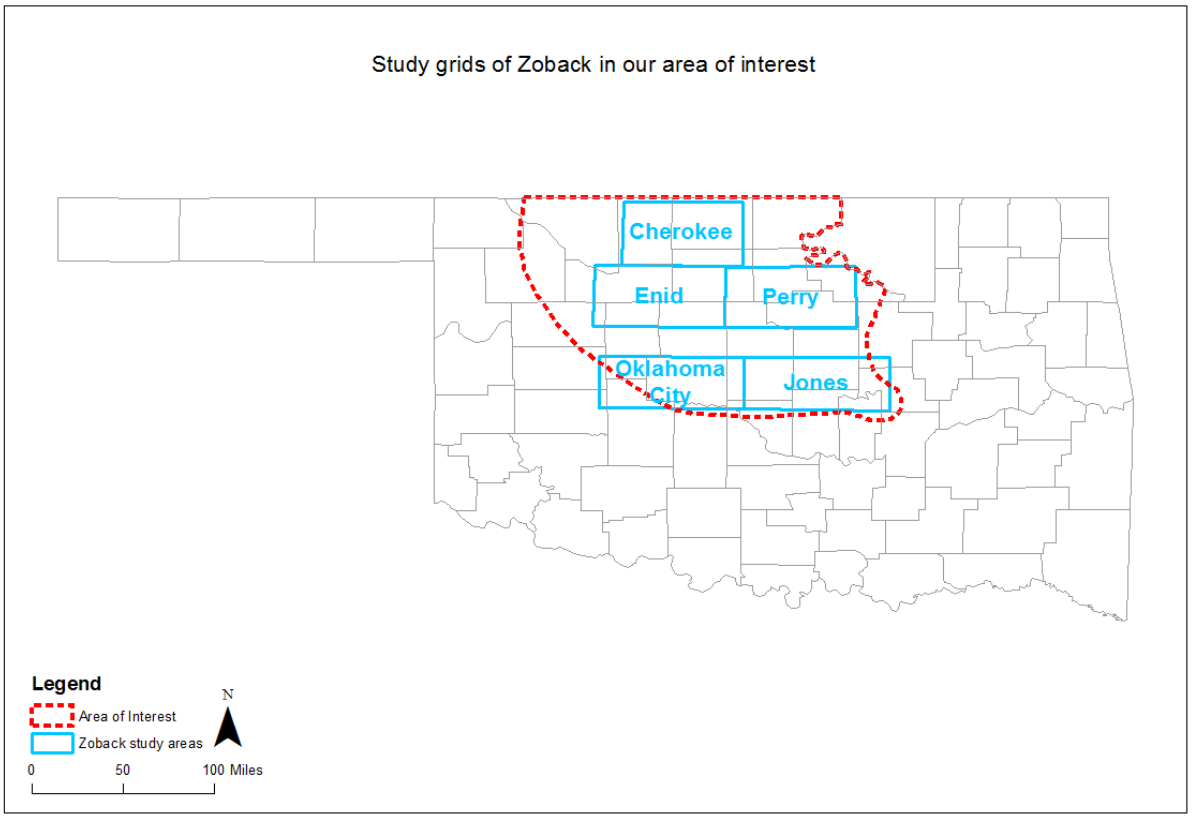

Figure 2: Area of interest

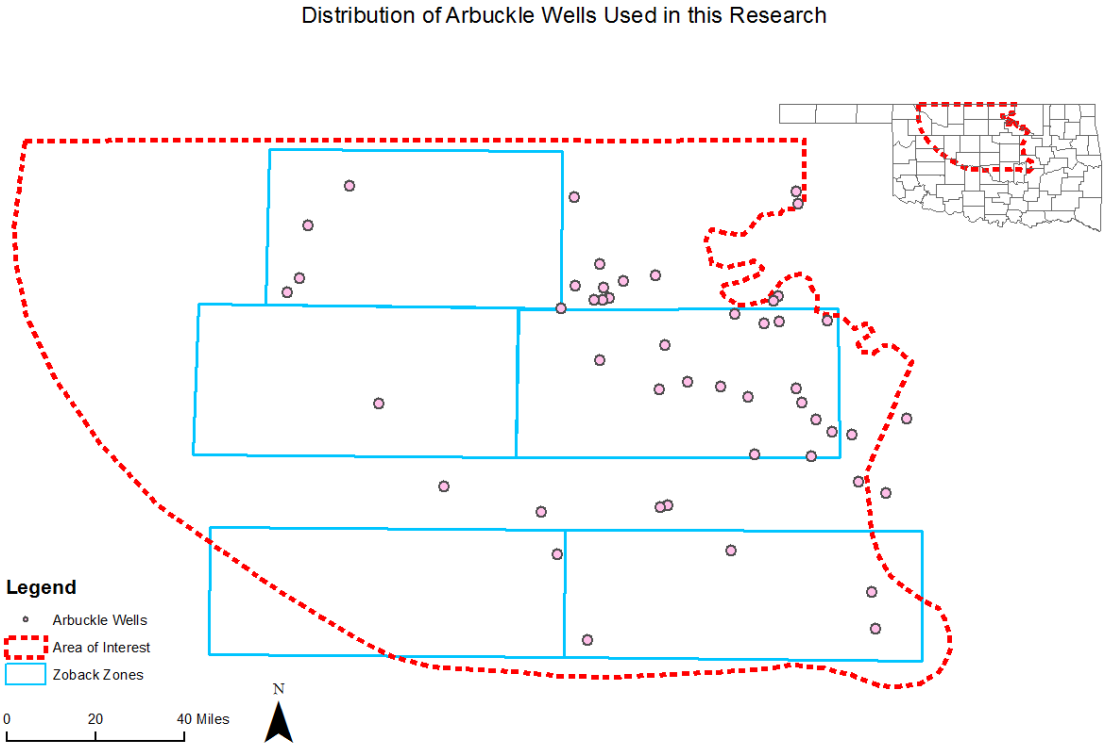

Figure 3: Arbuckle Wells to calculate Phi-H data

The distribution of our data points are not even (Figure 3). We have 46 wells, given by Brizendine (2016), for the Phi-H calculation in the Central region but only 9 usable wells in the Western region for Phi-H calculations. Earthquakes are clustered in three zones: Cherokee, Perry and a part of Jones. Injection wells are also unevenly distributed. For example, we have very few injection wells in the western half of the Enid zone, while we have a remarkable cluster of injection wells in the center of Oklahoma City zone (Figure 2).

VI) Methods and processing steps:

The basic method of our study is to conduct the spatial analysis based on different zones of our study area. Several types of zones were tested in our analysis, including Thiessen's polygons, squared grids with lateral length of 10 miles, squared grids with lateral length of 30 miles, squared grids with lateral length of 90 miles and grids defined by Walsh and Zoback (2015). We assigned attributes to each of those study zones in the following steps:

1. The number of earthquakes
    a. We archived earthquake data of the area of interest between 2012 and 2015 from the USGS website, and subdivided the file by year.
    b. We generated point shapefiles of earthquakes in each year and used the conversion tool in the ArcGIS (Point to Raster) to create a raster file in which ideally each earthquake will correspond to a pixel.
    c. In the setting of Point to Raster, we selected Count in the Cell Assignment Type drop bar so that if two or more earthquakes are too close to each other that we cannot turn them into different pixels, they would be merged into a single pixel but the value of that pixel would be the number of earthquakes at this place.
    d. Once we created the raster file of earthquakes, we applied the Zonal Statistics as Tables in the ArcGIS to count how many earthquakes are there in each study grid. The input field is the shapefile of our study grids and the value field is the raster file of earthquakes. This step gave us a table containing the total number of earthquakes occurred within a study zone during a single year. We could also get other statistical information such as the min, max, standard deviation and ranges.

e. We joined the Table created in Step 1.d. to the attribute table of our study grid shapefile.

f. We also used the Zonal Statistics as Tables to determine the maximum earthquake magnitude for each grid.

2. The injection volumes

. Original data of monthly injection volume are from the OCC website: http://www.occeweb.com/og/ogdatafiles2.htm. We assume that the unit of the injection volume is in US Barrel.

a. The injection volumes for each well are listed month by month. We used the OFFSET function in Microsoft Excel to SUM the injection volumes every 12 rows (corresponding to the months in a given year) and only kept one API number in every 12 rows. We copied those generated data to a new table file as the annual injection volumes of each well.

b. For each year, we join the annual injection volume table to the attribute table of All Wells based on the API number. Due to the large amount of data, the process in ArcGIS was too slow. Thus, we exported the attribute table and edited it in Excel.

c. We removed all wells that contained no information on injection data and kept all wells that had a value of zero or greater for injection volumes.

d. We added the edited table to ArcGIS and generated a new shapefile of injection volume in each year.

e. Then, we repeated what we did to the earthquake data to assign the injection volumes to each of our study grid. One difference was that in the setting of Point to Raster, we chose SUM instead of Count because we wanted to have total amount of injection water during that time.

3. The Phi-H data

. We had the list of basement wells in Oklahoma. We imported and clipped these wells with our area of interest.

a. There are total of 23 basement wells that are outside Travis area. MJ systems provided logs of 17 wells. We used LogSleuth and Petra to filter the wells which had bulk density logs or the neutron-density logs or both. We used neutron-density logs for porosity calculation because Arbuckle formation has many fractures so the sonic logs will not calculate the porosity correctly. The neutron tools must be calibrated for a given matrix lithology which is variable and the quality of neutron logs varies greatly between older logs and modern equipment.

b. In order to determine the top and base of the Arbuckle interval we used information of reported tops from IHS as well as an in house Excel spreadsheet located on the Shares drive which contained depths to the Arbuckle top and base. With this information we used our best judgment in correlating that top and base across the well logs of interest. After correlating we filtered the data to 9 wells with either bulk density logs or neutron-density logs and had a full section of the Arbuckle Group in the log.

c. We used Petra to digitize the bulk density logs and the neutron-density logs for wells that did not have the bulk density logs. We used two-foot intervals to extract the data from these logs in the Arbuckle Group.

d. We used the method of Brizendine (2016) to generate the Phi-H curves of these wells. For the wells that have bulk density logs, we calculated the neutron-density logs by the equation: =ma-bma-f. We used the dolomite density as our matrix density ma=2.85 g/ccand fresh-mud density f=1 g/cc (the value is from the Schlumberger well log handbook). Because the Arbuckle formation sometimes has sandstone layers within it, we used the quartz matrix density to substitute for dolomite matrix density in areas suspected of being sandstone. To determine

whether there are sandstone layers, we used the PE logs. The PE value of quartz mineralogy is 1.9-2.5, while it is 2.95-3.10 for dolomite. For the wells that only have the neutron-density logs, they usually are calibrated with limestone matrix. Therefore, we need to calculate the bulk density by the equation: b=ma-((ma-f)*) where limestone matrix density ma=2.71 g/ccand fresh-mud density f=1 g/cc (The value is from the Schlumberger well log handbook). Because Arbuckle formation is mostly dolomite, we calculated the neutron-density logs by equation =ma-bma-fwhere ma=2.85 g/ccand f=1 g/cc. We then calculated Phi-H for every two-foot interval by multiplying porosity by 2 (Figure 4).

e. Once we got Phi-H values of each well, we used the Kriging method to interpolate the Phi-H values across our study area. A raster file of Phi-H was created.

f. Then, we used the Zonal Statistics as Table tool to generate the table of the Phi-H values in each grid, and then we joined the table to the attribute of the grid shapefile.

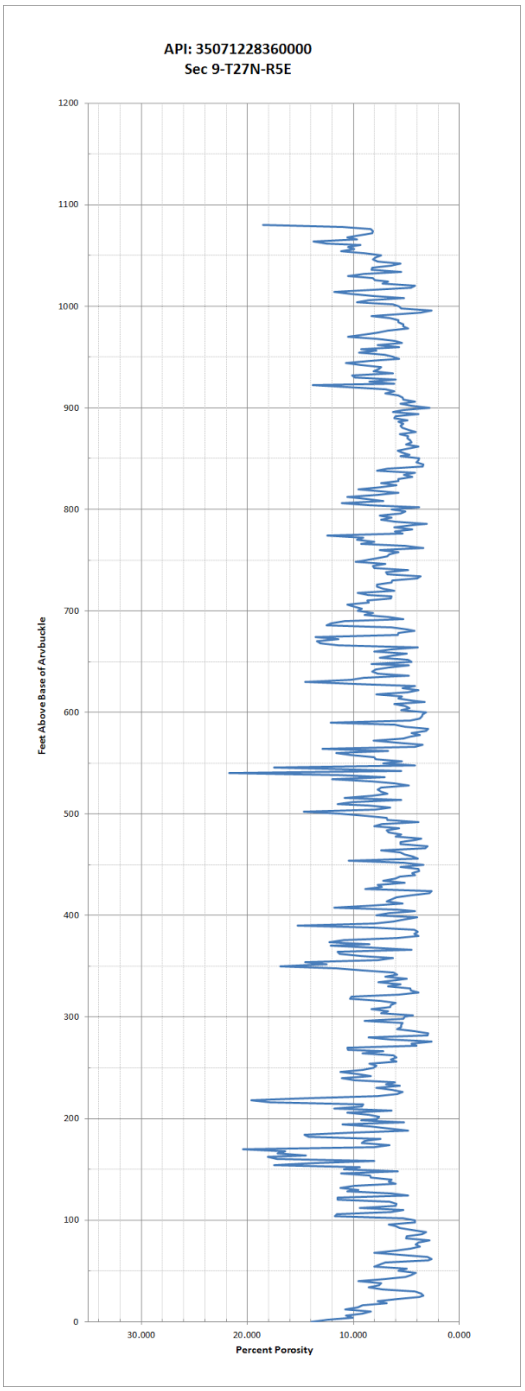

Figure 4: API: 35071228360000 Sec 9, T27N, R5E. Porosity Log. Y-Axis is thickness in feet above the base of the Arbuckle. X-Axis equal to percent porosity

4. The Phi-V data

a. A new field was added to the shapefile of study grids in order to add values of areas.

b. We defined the coordinate system of the data frame into State Plane Oklahoma North US Feet which is a projected coordinate system because we could not do the field geometry calculation under a geographic coordinate system. Under this projection, we calculated the area of each grid in cubic feet.

c. We re-defined the coordinate system back to the original system (NAD 83).

d. We multiplied Phi-H by the area of each grid to get the Phi-V in cubic feet.

e. We then converted Phi-V in cubic feet to US barrels by multiplying by 0.178.

5. The ratio injection/phi-V:

    a. The idea behind this ratio is that we wanted to determine how much pore space had been filled with injection water per year.

    b. We also want to examine the combined effect of injection volume and the total porosity on the earthquakes. The ratio between injection volume and the Phi-V can indicate what portion of the pore space in the rock is filled with injected wastewater, and it would be interesting to see if there were any correlation between that ratio and the number of earthquakes..

    c. If we can find the ratio value where many of earthquakes happened, we can determine the suitable volume of injection in different areas.

V) Analysis:

1. **Regression of 10 * 10 Grids in Perry:**

We used the same Ordinary Least Squares regression analysis method to analyze the Perry area defined by Zoback's zones. The dependent variable for this analysis is the number of 2015 earthquakes, while the independent variable is the ratio between the injection volume and Phi-V.

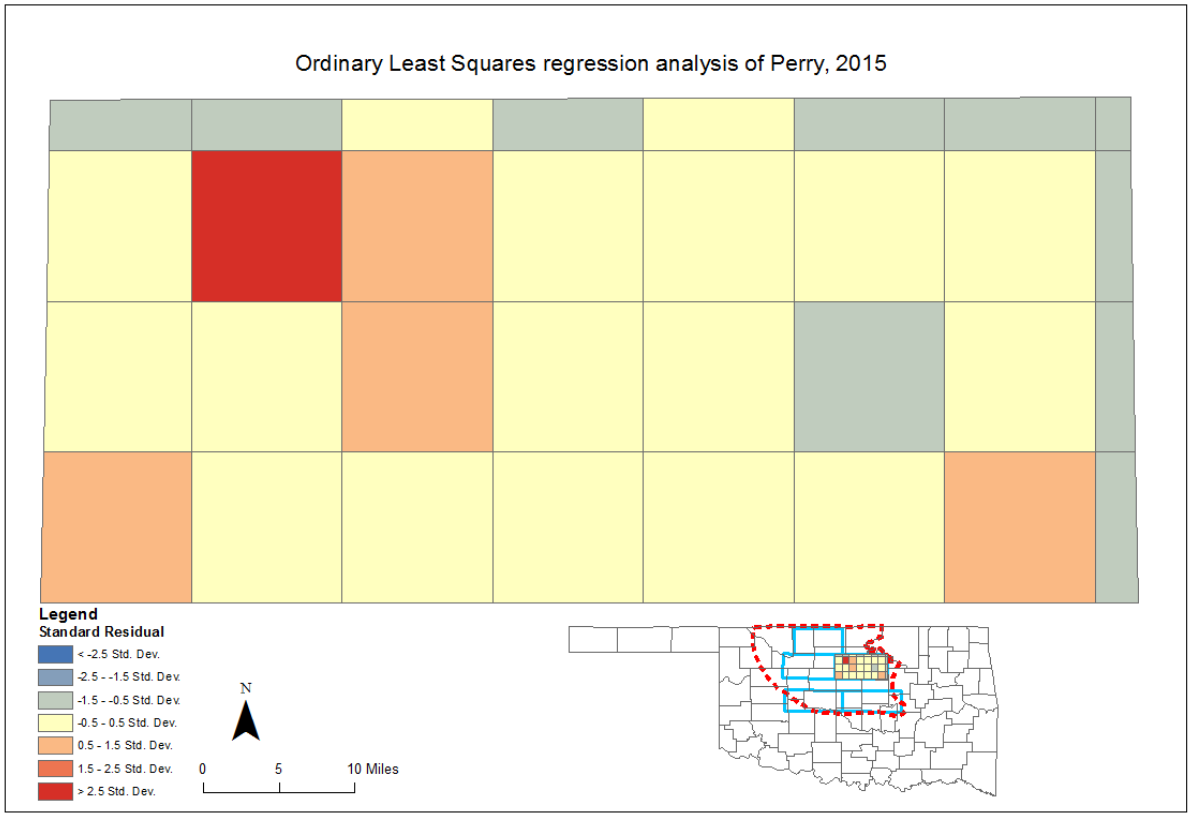

Figure 5: Area of interest 10 * 10 grids in Perry linear regression standard residual between number of earthquake and injection volume, phi-H, thickness

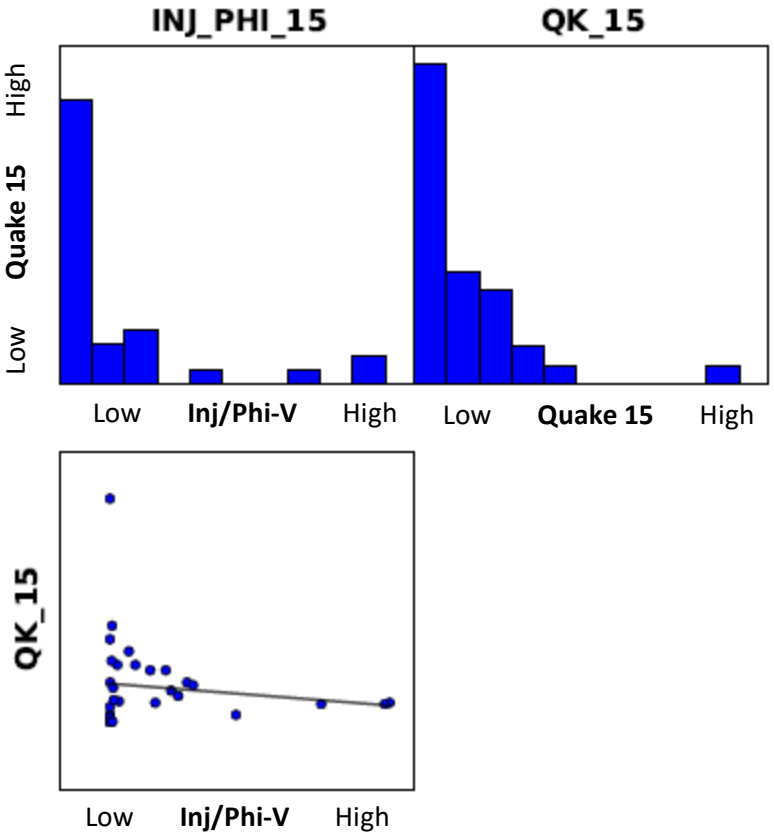

Figure 6: Perry 10 * 10 grids linear regression between number of earthquake and (Injection volume/Phi-V)

In this case, we found a slightly negative trend between the number of earthquake and the ratio between injection volume and the Phi-V, which does not make any sense because a higher injection/Phi-V ratio should lead to a higher number of earthquakes (Figure 5 & 6). Therefore, we decided to use bigger grids so that more injection and earthquake data could be in the same grid, and that might help improve our analysis.

2) Regression of 40 * 40 Grids:

After setting up the data, we conducted the Ordinary Least Squares regression analysis based on the 40-mile grids for each year. The dependent variable of our analysis was number of

earthquakes in each year, and independent variables include injection volume, Arbuckle thickness and Phi-H.

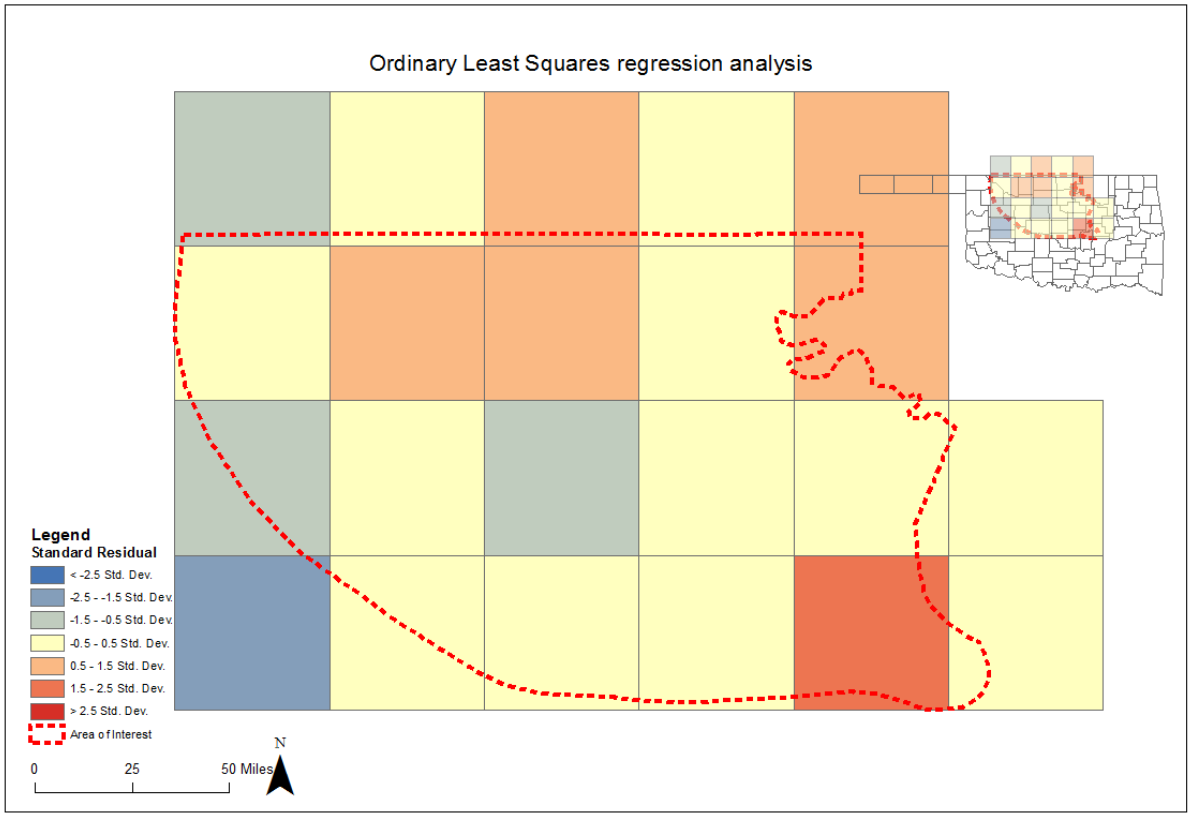

Figure 7: Area of interest 40 * 40 grids linear regression standard residual between number of earthquake and injection volume, phi-H, thickness

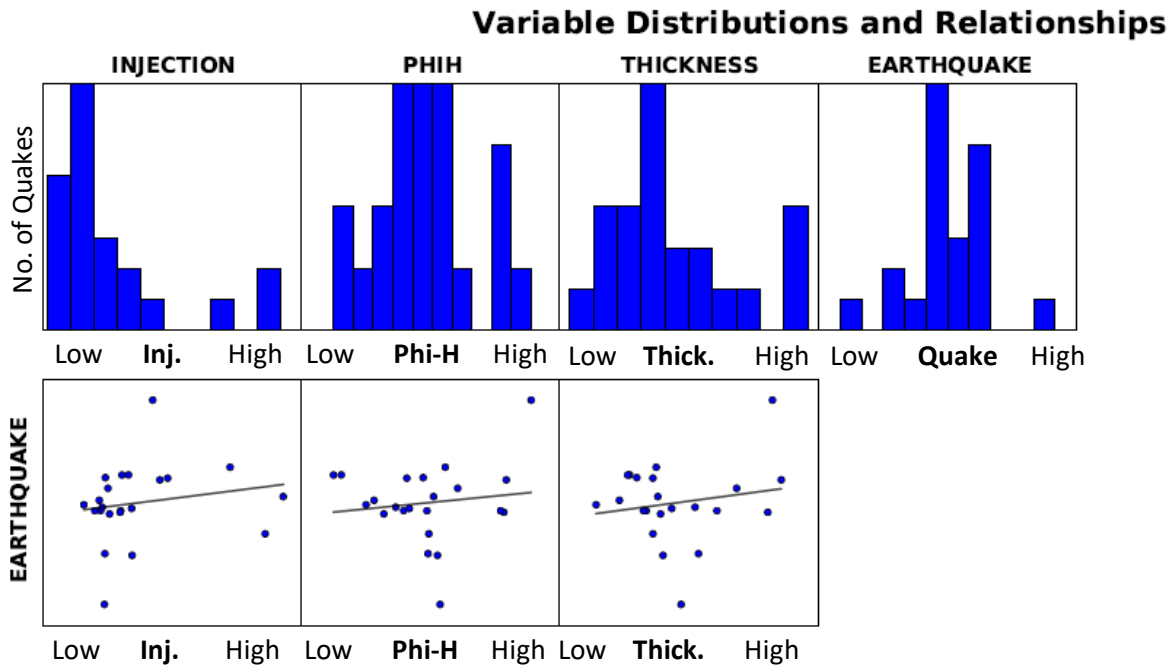

Figure 8: Area of interest 40 * 40 grids linear regression graph between number of earthquake and injection volume, phi-H, thickness

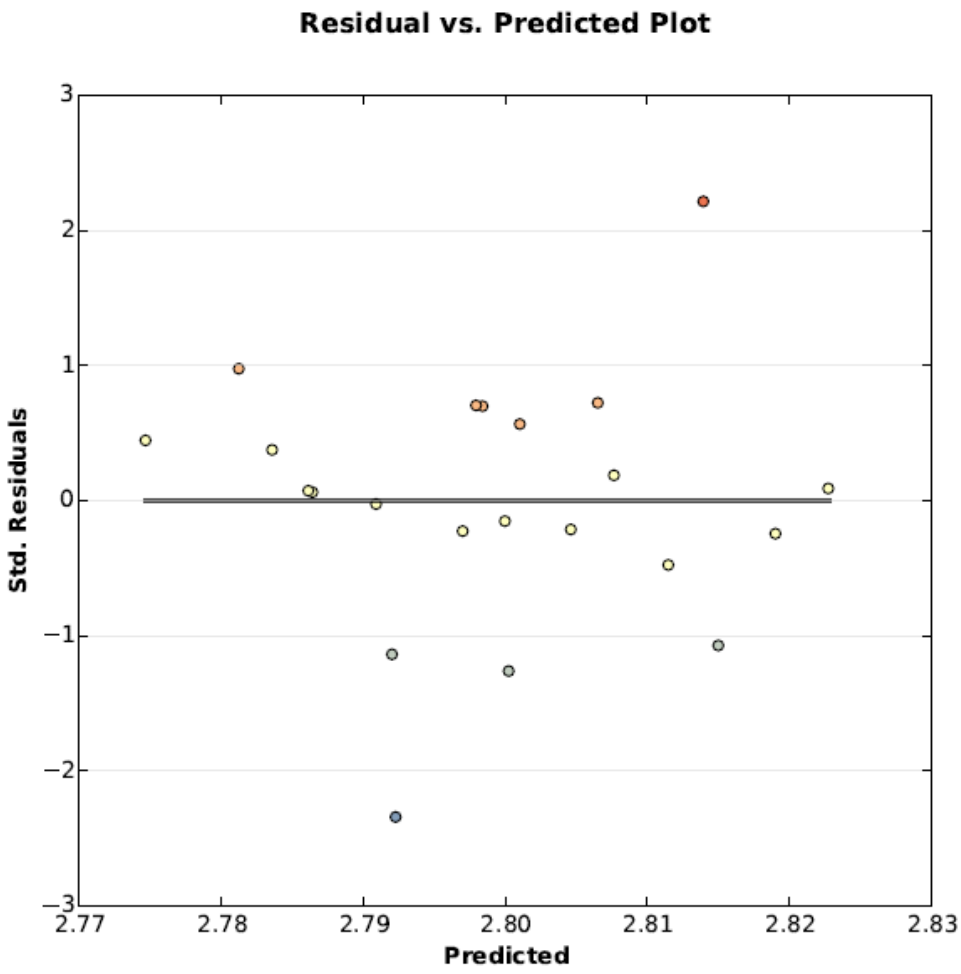

Figure 9: Area of interest 40 * 40 grids linear regression distribution between number of earthquake and injection volume, phi-H, thickness

The result shows a random distribution (Figures 7, 8 and 9). It does not make sense that earthquakes focus in the area with low injection volume. So we thought of lag distance between earthquakes and injection volume.

Then, we plotted earthquakes and injection volumes on the same map (Figure 10). Based on the map, we then suspect that there should be a lag distance between the injection volumes and the

center of earthquakes. For example, the cluster of earthquakes in the C4 and D4 might be induced by injections in C5 and D5. Therefore, we decided to conduct a Hot Spot Analysis to see the general spatial lag distance between earthquakes and injection volumes.

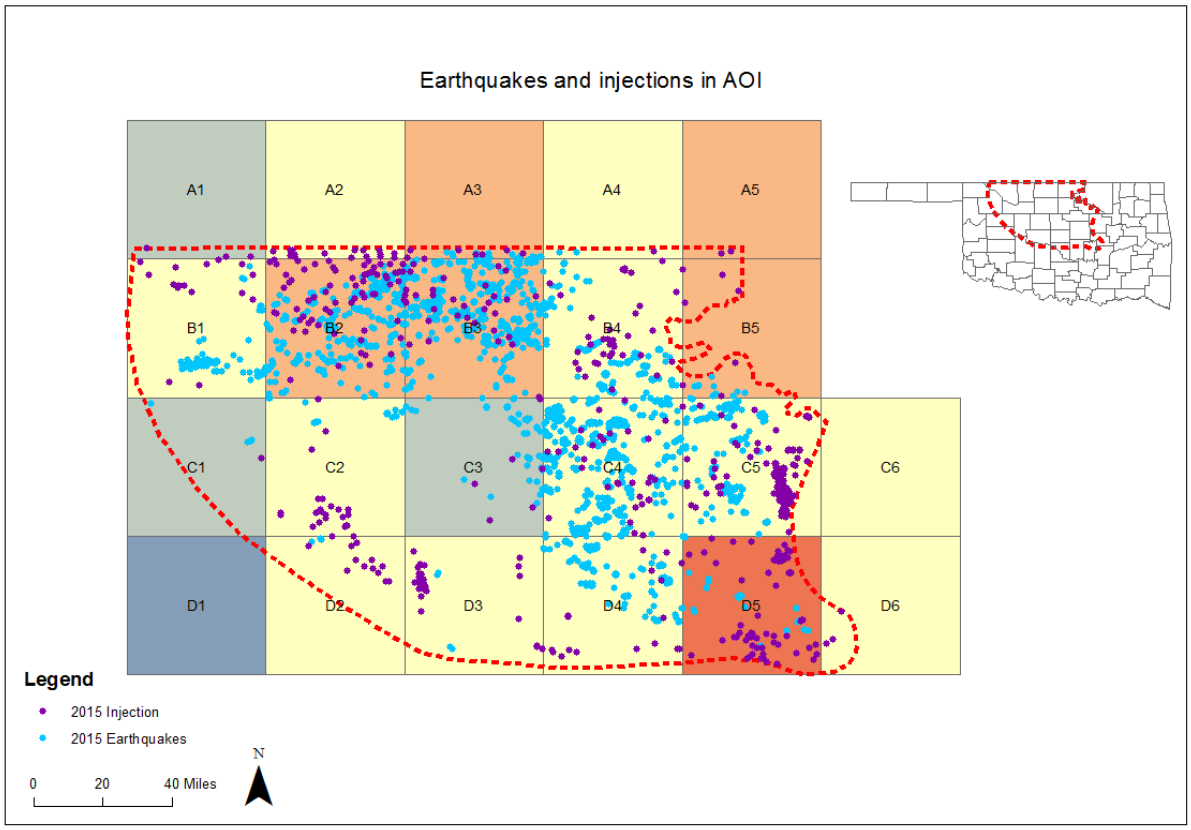

Figure 10: Area of interest 40 * 40 grids with earthquakes and injection sites

3) Hot Spot Analysis (the Getis-Ord Test, or the G-Test):

To identify the potential lag distance between the injection wells and induced earthquakes, we conducted the Hot Spot Analysis with 10 * 10 Grids to find out how the injection volumes and earthquakes are distributed in space compared to each other. Two different methods were used to define neighbors in the conceptualization of spatial relations during the Hot Spot Analysis:

- Inverse Distance Squared (Closer polygons in the space will have stronger influences between each other) with Euclidean Distance
- Queen's contiguity (Polygons sharing any edges or cornors would be considered as neighbors)

According to our analysis, the results of Inverse Distance Squared method, which is based on the true distance, show neither significant hot spots nor cold spots for injection volumes. Some minor hot spots shown on the map could not truly reflect the distribution of our injection data. In this case, although the Inverse Distance Squared method was able to identify pretty good hot spots for our earthquake data, we decided to use the Queen's contiguity method in this analysis.

There are two hot spots of injection volumes in 2015 (Figure 11). The northwestern hot spot is located in the Alfalfa and Woods counties, and the eastern hot spot is mainly located around the borders between Creek, Payne and Lincoln counties.

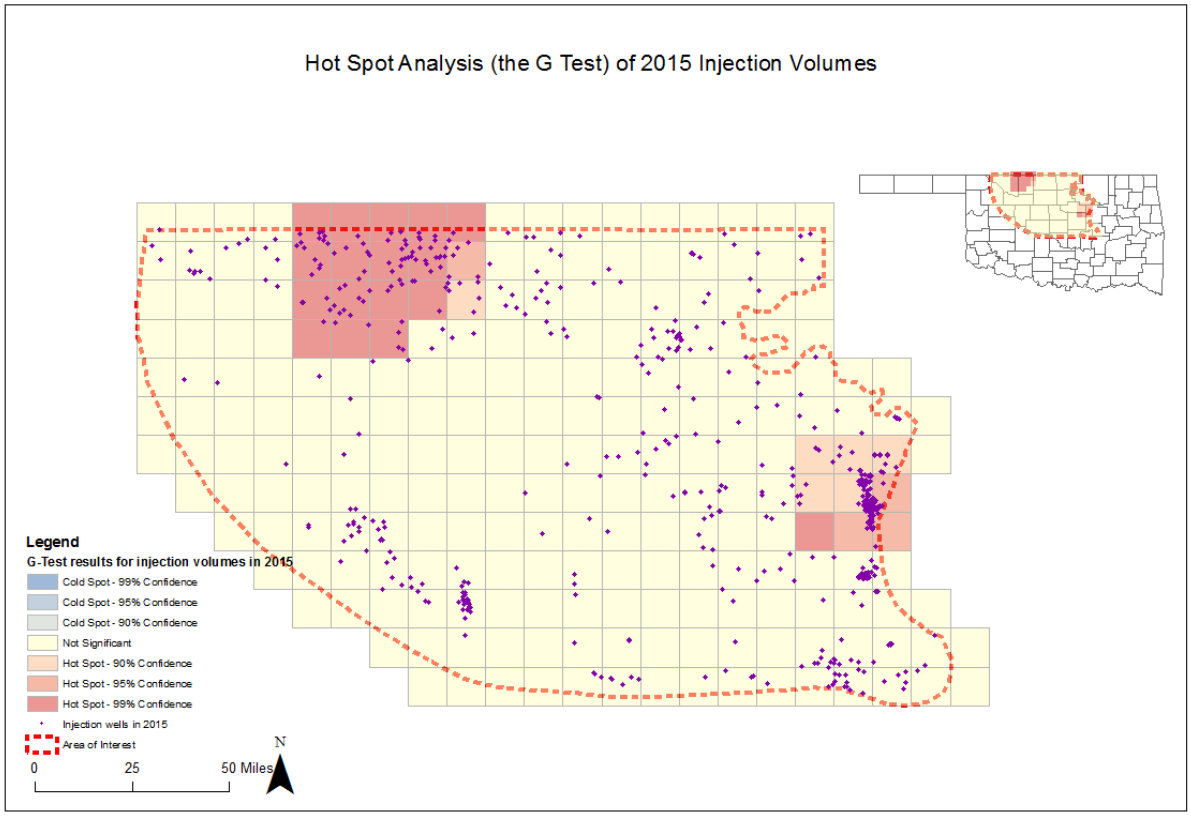

Figure 11: Hot spot analysis of 2015 injection volume

There are also two hot spots of earthquakes in 2015 (Figure 12). The northwestern earthquake hot spot of 2015 is centered in the Grand county and extends into Alfalfa county. The southeastern hot spot is centered in Logan county and extends into Garfield, Noble and Payne counties.

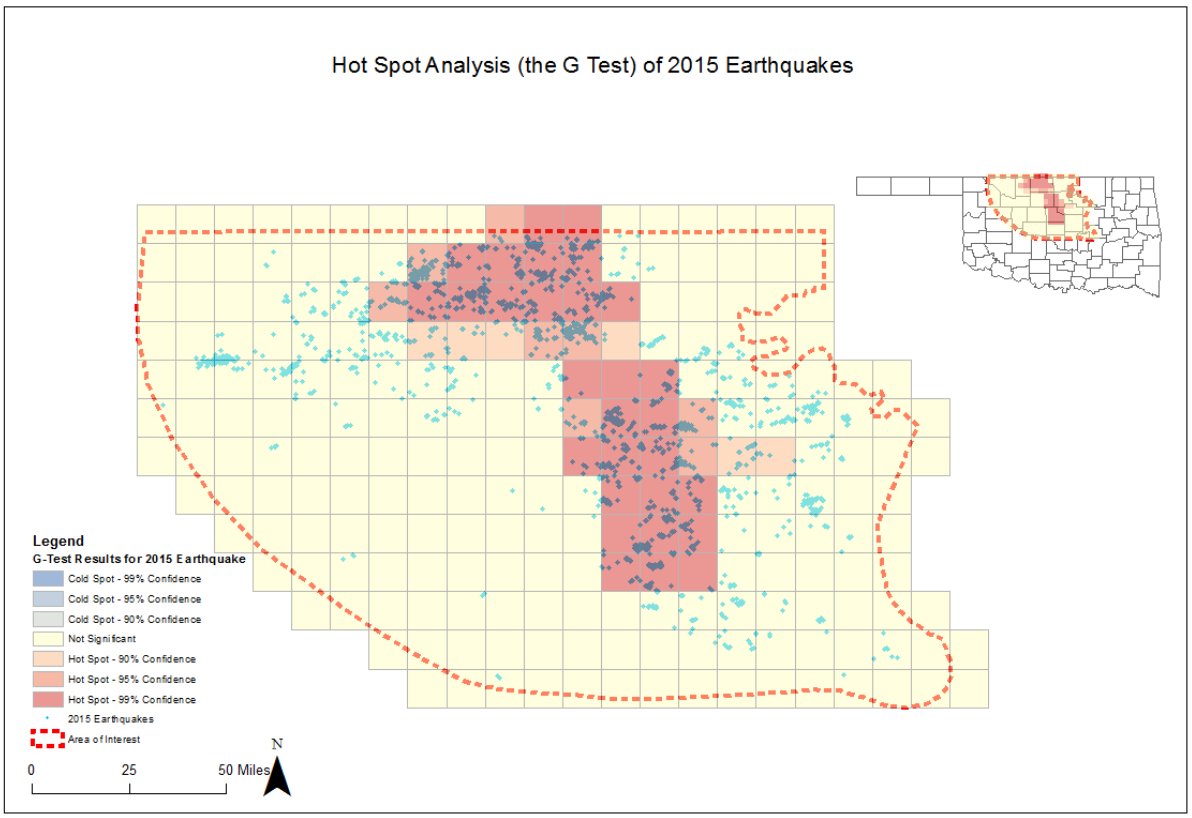

Figure 12: Hot spot analysis of 2015 earthquakes clusters

We plot the 2015 earthquake hot spots and injection hot spots on the same map in order to identify the potential lag distance between the injection volumes and earthquakes (Figure 13). From this plot, we can see that earthquake clusters are relatively closer to the Nemaha Fault Zone compared to the locations of injection hot spots. The lag distance between injection volume and earthquakes can be determined by checking the distance between the center of hot spots. The lag distance in this case would be about 30 - 40 miles. However, we are not sure about the

significance of tectonic activities.

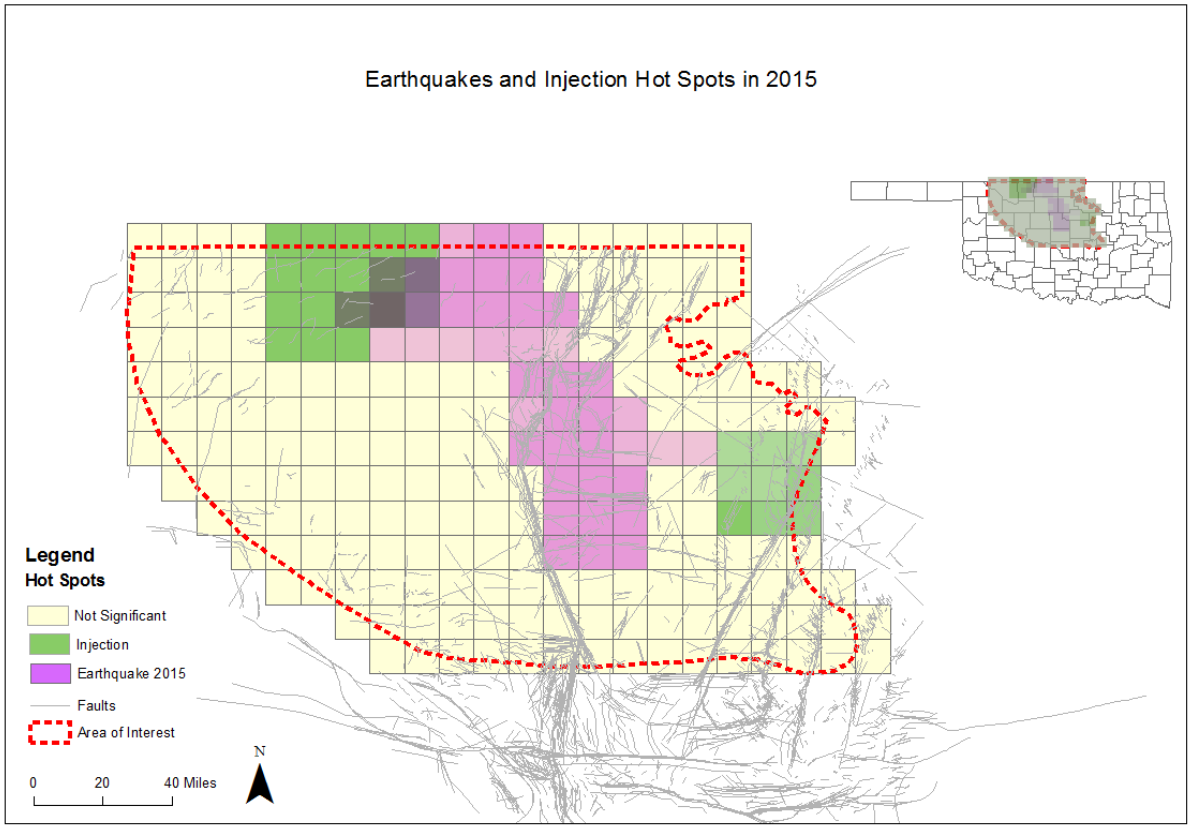

Figure 13: Comparison of hot spots of injection volume and earthquakes in 2015

We also did the Hot Spot Analysis on the Phi-H distribution in our study area (Figure 14). From this result, we can see a clear hot spot as well as a cold spot of the Phi-H. According to the map of fault distribution in Figure 15, Phi-H is high near major structural features such as Cushing Anticline or Nemaha Fault.

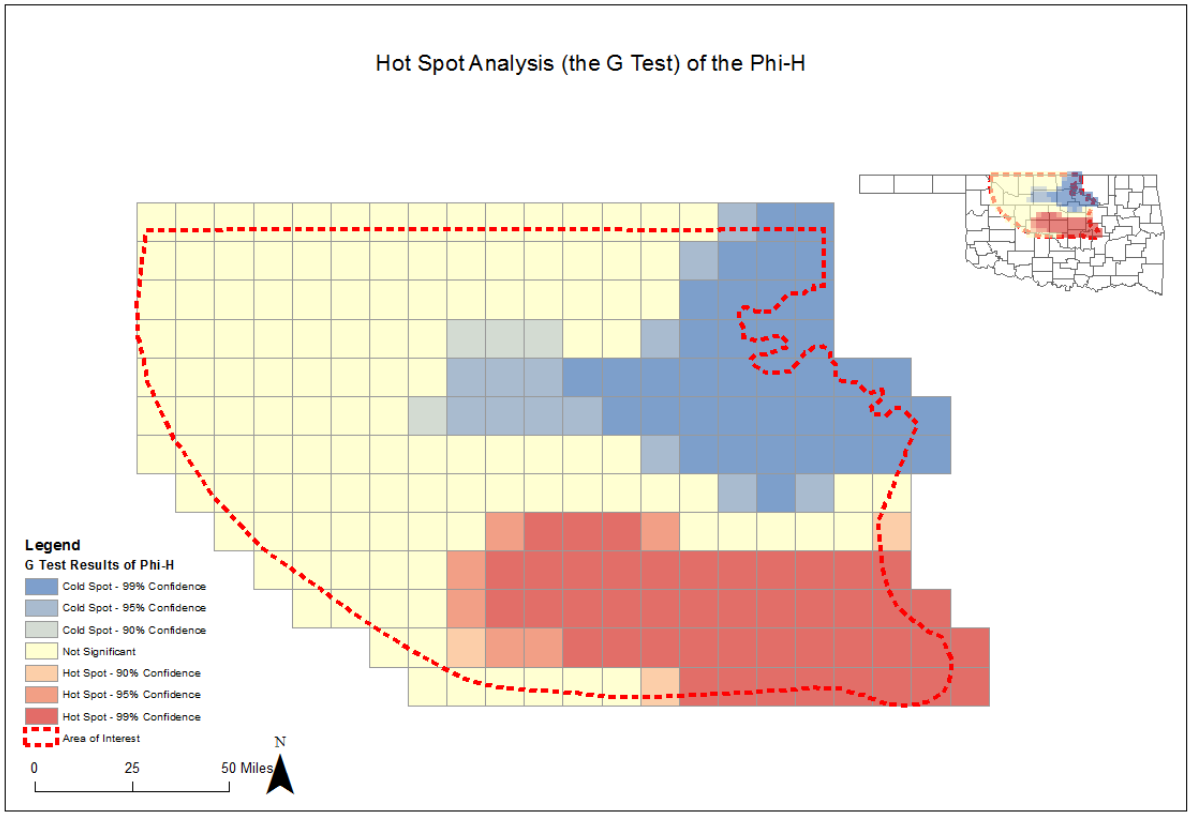

Figure 14: Hot spot analysis of Phi-H

Figure 15: Phi-H distribution and faults

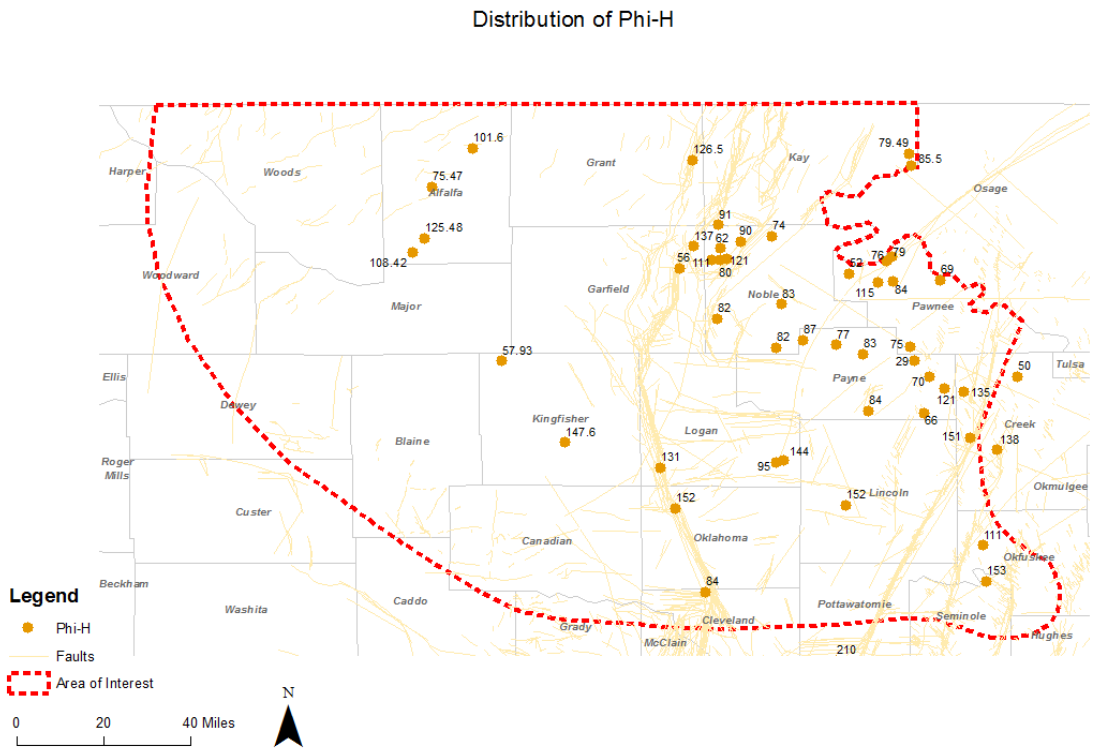

We made a plot of the Phi-H hot spots and 2015 injection volume hot spots on the same map to identify the risky areas (Figure 16). According to this map, the area between Payne, Creek and Pawnee counties has a hot spot in 2015 injection volume, while it is also located close to a cold spot of Phi-H value which indicates a low porosity zone. Therefore, the risk of earthquake in that region should be higher. The 2016 Pawnee and Cushing earthquakes might partially illustrate the high risk of this region.

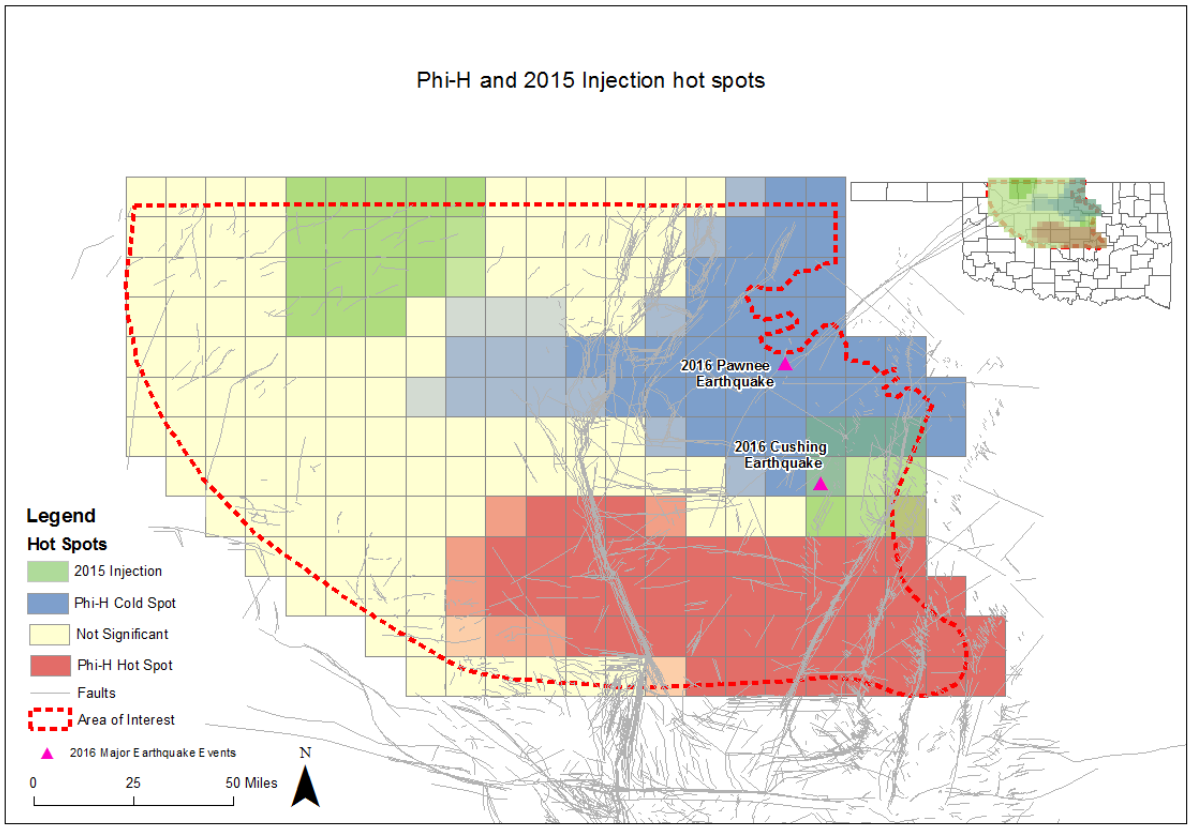

Figure 16: Phi-H and 2015 injection spatial distribution

VI) Results:

1. The relationship between Arbuckle thickness and Phi-H value:

We created a plot of Phi-H versus Arbuckle thickness (Figure 17). Except for one outlier of well API 3507324081 in Section 9, T27N, R5E, other data follow almost the same linear equation that Travis suggested in his thesis: $y = 0.056x + 18.976$. It is obvious that Phi-H value increases with the increase of Arbuckle thickness. The variety of Phi-V values with the same Arbuckle thickness indicates the anisotropy and heterogeneous properties of Arbuckle formation.

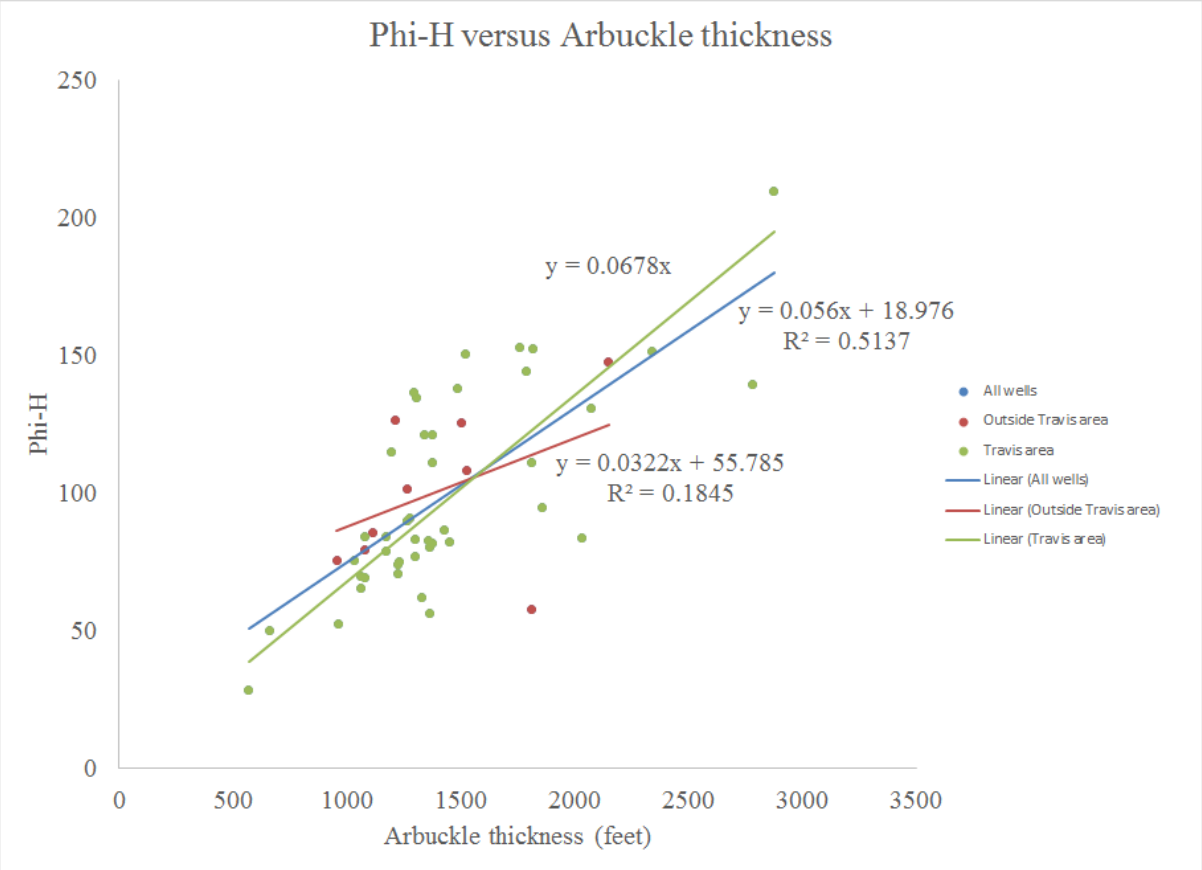

Figure 17: Phi-H versus Arbuckle thickness graph

2) Phi-V analysis:

After calculating the ratio between injection volume and Phi-V, we recognized that the injection volume accounts for only small part of total porosity of Arbuckle formation.

We studied the ratio between injection volume and Phi-V for each year between 2012 and 2015 and how they relate to the number of earthquakes in each of those 5 Zoback zones. We have a total of 20 data points of 4 years in 5 different zones, and we plot them in these following charts:

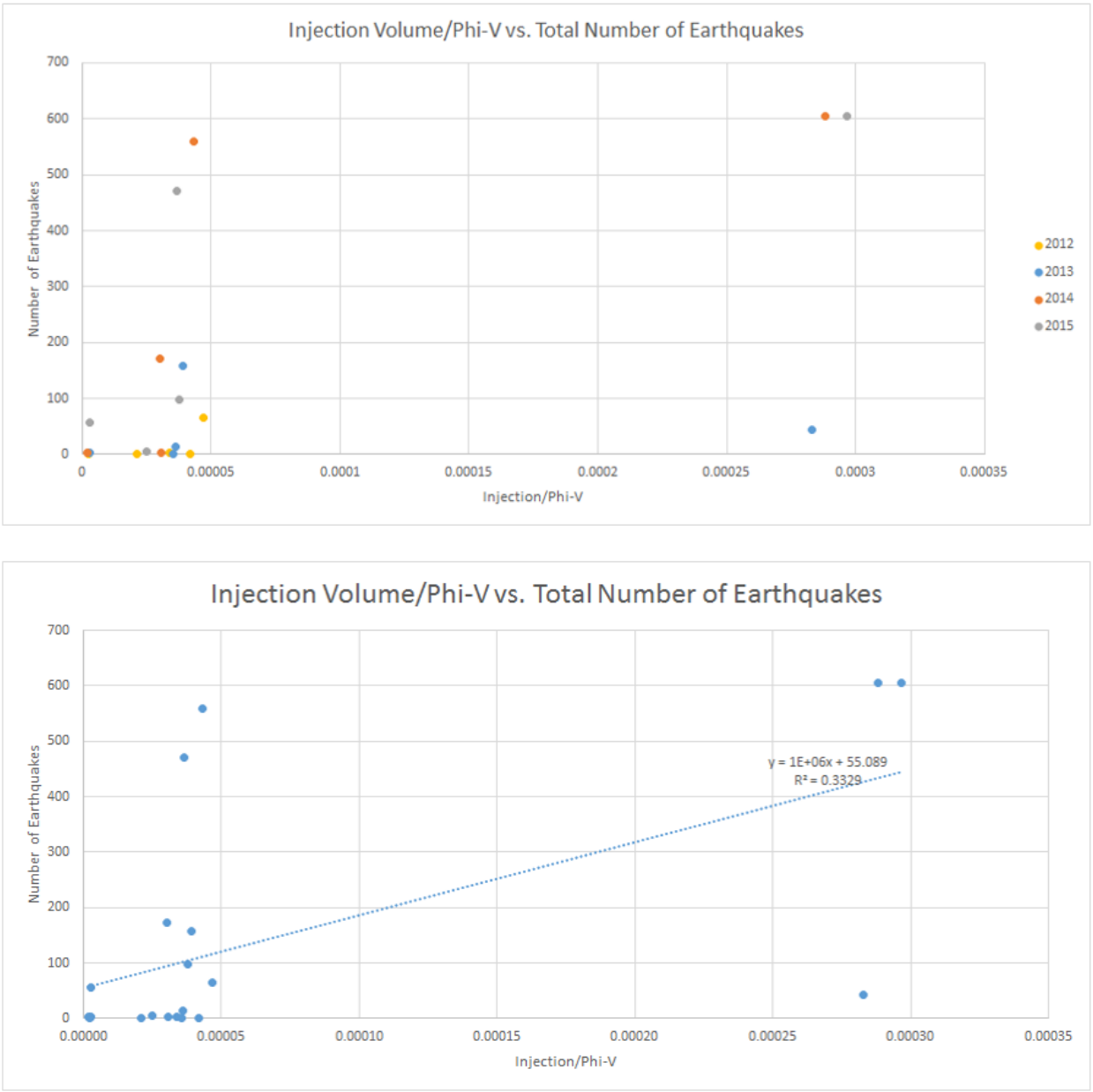

Figure 18: Total number of earthquakes versus (Injection Volume/Phi-V)

There is a general positive relationship between the Injection/Phi-V and the number of earthquakes. However, the relationship is not very strong. The R2 of the linear trend line is only about 0.3329. A clear outlier occurs in the Cherokee zone in 2013. During that year, the injection volume at Cherokee was high, but the number of earthquakes in the corresponding

region in the same year was relatively low. Outliers are also in Perry zone where the numbers of earthquakes were significantly higher than what the linear trend line predicted in 2014 and 2015. This might due to the fact that Perry has the highest number of faults within it compared to other zones and is located right next to the Nemaha Fault Zone. Some of those earthquakes may have been generated by natural tectonic processes rather than the injected wastewater.

We also tested the relationship between the number of earthquakes of each zone and the ratio between the cumulative injection volumes over Phi-V (Figure 19).

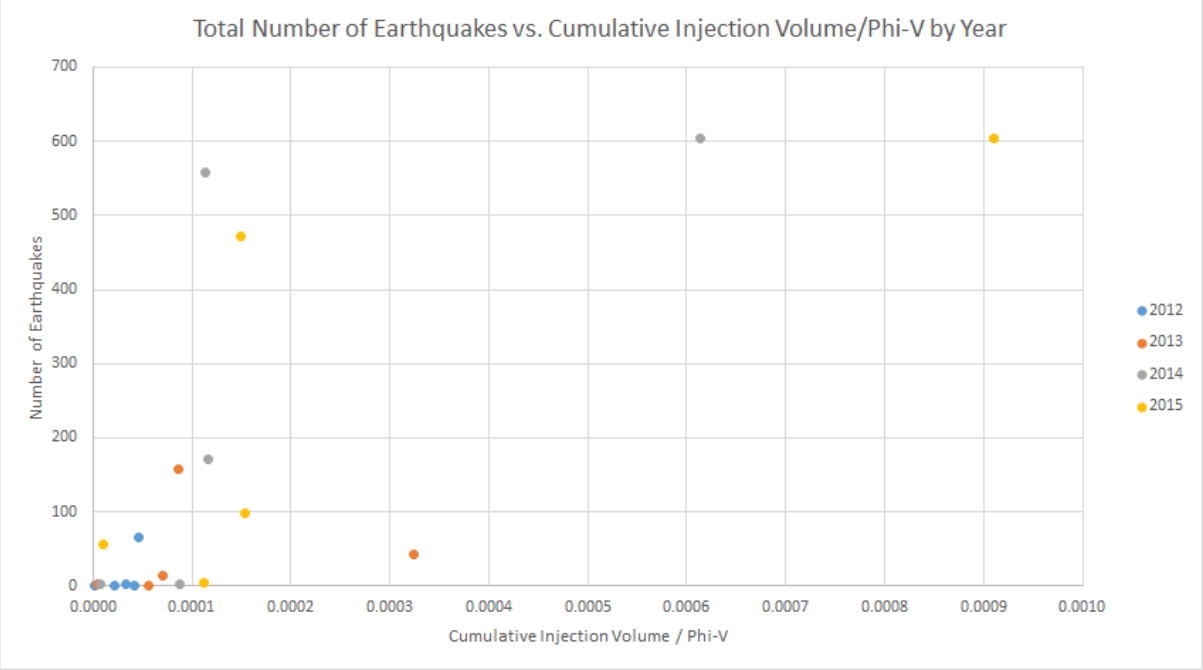

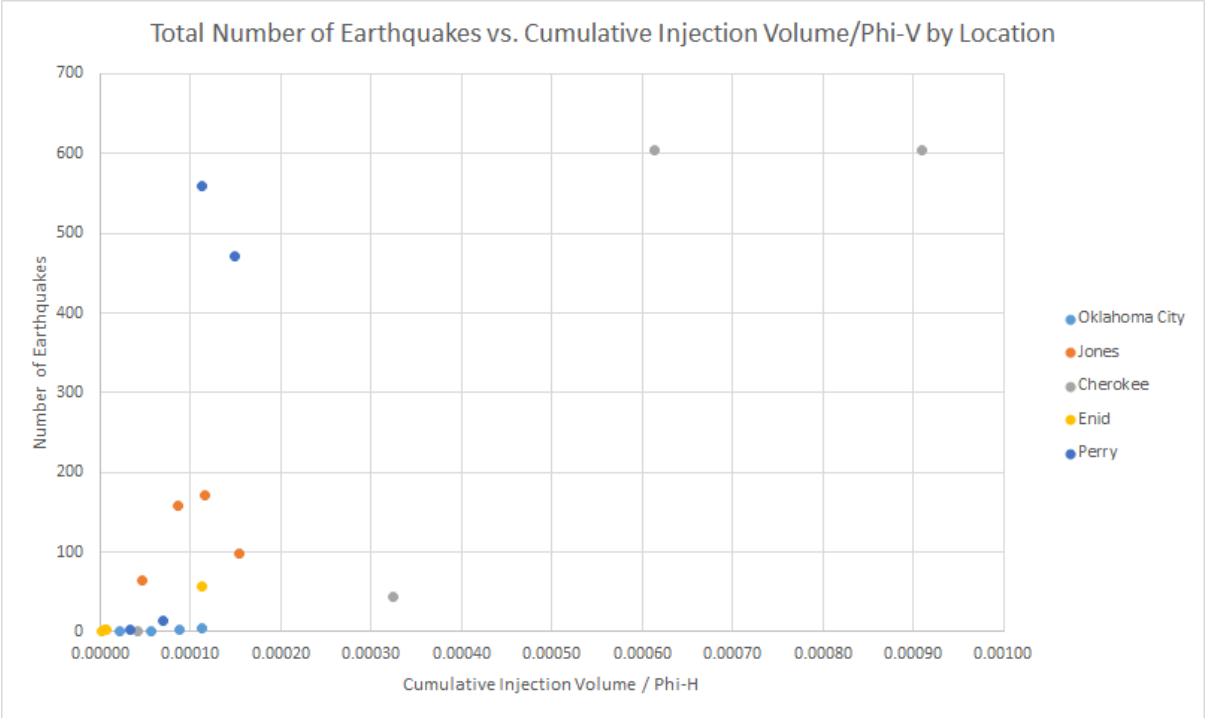

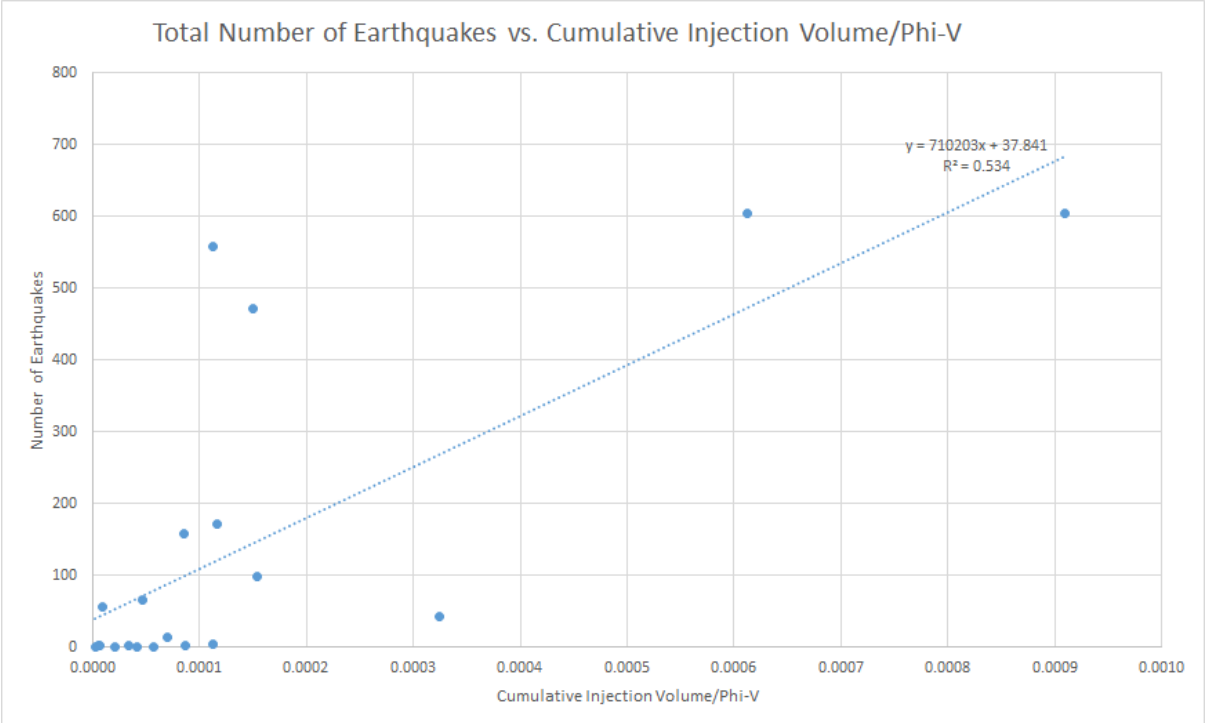

Figure 19: Total number of earthquakes versus (Cumulative Injection Volume/Phi-V)

The cumulative injection volume is the sum of injection volumes from 2012 to 2015 in that region. In this case, the R2 of the linear trend line is significantly higher than the previous R2 of non-cumulative injection volumes (Figure 20). It means that the wastewater accumulates in a “pressure cone” in the vicinity of the wells. The greater the amount of total injection, the greater the pressure is, and the greater the likelihood of earthquakes.

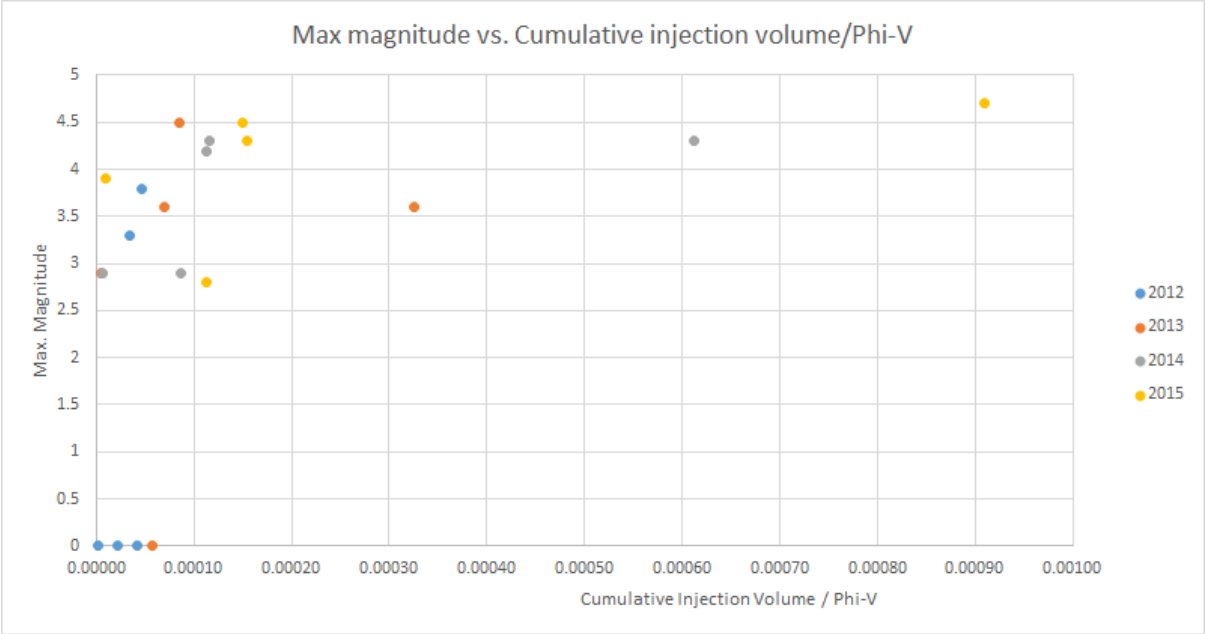

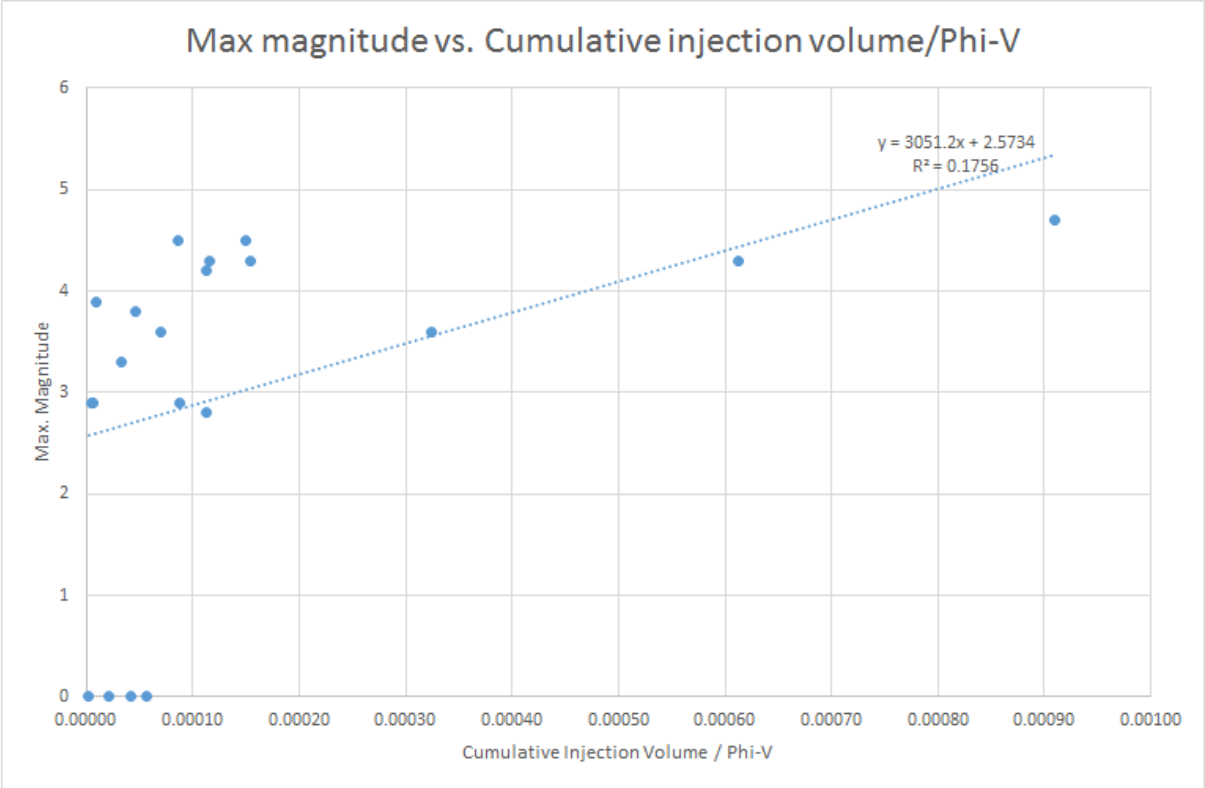

Figure 20: Maximum magnitude of earthquakes versus (Cumulative Injection Volume/Phi-V)

There is a linear relationship between maximum magnitude of earthquakes and the ratio (Cumulative Injection Volume/Phi-V). However, because of lacking data, we did not have the high correlation.

VII) Conclusion:

1. There is a linear relationship between Phi-H value and Arbuckle thickness in our area of interest. However, with the same arbuckle thickness, the Phi-H value will vary. It shows that the Arbuckle formation is anisotropic and heterogeneous. The Phi-H value is high near some major structural features such as the Nemaha Fault.
2. There is a lag distance of 30-40 miles between the injection wells and earthquakes.

3. The injection volume is still small compared to the total porosity of Arbuckle formation, but it causes earthquakes. The potential explanation is that the formation of Arbuckle is already saturated with fluid and considerably pressured. If the pore spaces in the Arbuckle formation were already filled with other fluids and the formation was already pressured, it would be more sensitive to additional volumes of water injected and the formation would be over-pressured more easily.
4. There is a linear relationship between total number of earthquakes and the ratio (Cumulative Injection Volume/Phi-V). The correlation is better when we used the cumulative injection volume. It means that the wastewater accumulates around the wells, which causes greater pressure and greater possibility of earthquakes. There is also a linear relationship between maximum magnitude of earthquakes and the ratio (Cumulative Injection Volume/Phi-V).
5. Lacking data is the main problem of this project. The distribution of data also causes challenges in doing the statistical analysis. We expect to have more data in order to have higher correlation and to determine the best ratio of safe injection volume over Phi-V in our area of interest.

References

Walsh Zoback 2015

Brizendine 2016

Langenbruch, C., and M. D. Zoback, 2016, How will induced seismicity in Oklahoma respond to decreased saltwater injection rates?: Science Advances, v. 2, no. 11

Mcnamara, D. E. et al., 2015, Efforts to monitor and characterize the recent increasing seismicity in central Oklahoma: The Leading Edge, v. 34, no. 6, p. 628–639

Walsh, F. R., and M. D. Zoback, 2015, Oklahoma's recent earthquakes and saltwater disposal: Science Advances, v. 1, no. 5

Eardley, A. J., 1951, Structural geology of North America: New York, Harper and Brothers.

Berryhill, R. A., 1961, Subsurface geology of south-central Pawnee County, Oklahoma: Oklahoma City Geological Society Shale Shaker, v. 12, no. 4, p. 2-18.

Northcutt, R. A., and Campbell, J. A., 1995, Geologic Provinces of Oklahoma: Oklahoma Geological Survey Open-File Report OF5-95

Johnson, K.S., 2008. Geologic history of Oklahoma. Earth sciences and mineral resources of Oklahoma: Oklahoma Geological Survey Educational Publication, 9, pp.3-5.

Huffman, G. G., 1958, Geology of the south and west flanks of the Ozark uplift, northeast Oklahoma: Bulletin - Oklahoma Geological Survey, vol. 77, p. 27- 41.